horticulturae

MDPI

Article

Characteristics and Comparative Analysis of the Complete Plastomes of *Apostasia fujianica* and *Neuwiedia malipoensis* (Apostasioideae)

Qinyao Zheng [1], Yuwei Wu [1], Shi-Jie Ke [2], Ding-Kun Liu [3] and Zhong-Jian Liu [1,2,*]

[1] Key Laboratory of National Forestry and Grassland Administration for Orchid Conservation and Utilization at Landscape Architecture and Arts, Fujian Agriculture and Forestry University, Fuzhou 350002, China; qinyaozheng@fafu.edu.cn (Q.Z.); 1211775050@fafu.edu.cn (Y.W.)
[2] College of Forestry, Fujian Agriculture and Forestry University, Fuzhou 350002, China; 3210422027@fafu.edu.cn
[3] College of Life Science, Jinggangshan University, Jinggangshan 343000, China; liudingkun@jgsu.edu.cn
* Correspondence: zjliu@fafu.edu.cn

Abstract: Apostasioideae, the early divergent subfamily of Orchidaceae, comprises *Apostasia* and *Neuwiedia* genera with approximately 20 species. Despite extensive research on Apostasioideae, previous studies have struggled to resolve taxonomic issues, particularly concerning the position of species within this subfamily. Here, we sequenced and annotated plastomes of *Apostasia fujianica* and *Neuwiedia malipoensis*, unveiling their phylogenetic relationships and shared plastome features with the other five published plastomes. We identified and analyzed the length, GC content, repeat sequences, and RSCU values of the chloroplast genomes. It is noteworthy that the chloroplast genome of *N. malipoensis* stands out as the largest among all known chloroplast genomes within the Apostasioideae subfamily, primarily due to contributions from both the LSC and SSC regions. Furthermore, our analysis revealed three unique structural rearrangements located approximately 10k–47k bp (*ycf3–trnS-GCU*) and 58k–59k bp(*accD*) in the LSC region and 118k–119k (*ndhI*) bp in the SSC region of the chloroplast genomes across all five species within the *Apostasia* genus, which presents a potential avenue for identifying distinctive chloroplast genetic markers, setting them apart from other orchid plants. And a total of four mutational hotspots (*rpoC2*, *atpH*, *rps4*, *ndhK*, and *clpP*) were identified. Moreover, our study suggested that *Apostasia* and *Neuwiedia* formed a monophyletic group, with *Apostasia* being sister to *Neuwiedia*. Within the *Apostasia* genus, five species were classified into two major clades, represented as follows: (*A. odorata* (*A. shenzhenica* and *A. fujianica*) (*A. ramifera* and *A. wallichii*)). These findings hold significance in developing DNA barcoding of Apostasioideae and contribute to the further phylogenetic understanding of Apostasioideae species.

Keywords: phylogenetic analysis; structural rearrangement; Orchidaceae

Citation: Zheng, Q.; Wu, Y.; Ke, S.-J.; Liu, D.-K.; Liu, Z.-J. Characteristics and Comparative Analysis of the Complete Plastomes of *Apostasia fujianica* and *Neuwiedia malipoensis* (Apostasioideae). *Horticulturae* **2024**, *10*, 383. https://doi.org/10.3390/horticulturae10040383

Academic Editor: Jong-Wook Chung and Sebastin Raveendar

Received: 6 March 2024
Revised: 29 March 2024
Accepted: 5 April 2024
Published: 10 April 2024

1. Introduction

The orchid family is the most diverse group of flowering plants among the angiosperm monocotyledons (>40% of all monocotyledons) [1], comprising over 28,000 known species across 763 genera [2]. Previous DNA molecular studies have classified the orchid family into five subfamilies: Apostasioideae, Vanilloideae, Cypripedioideae, Orchidoideae, and Epidendroideae [3]. Apostasioideae, a terrestrial, species-poor subfamily of Orchidaceae, comprises only two genera (*Apostasia* and *Neuwiedia*) with about 20 species [4]. Acknowledged as the earliest diverging lineage of Orchidaceae and often considered the most primitive group of extant orchids [5], Apostasioideae species serve as a crucial outgroup for evolutionary studies across all other orchid subfamilies.

Due to the distinct morphological features, there have been differences of opinion about the taxonomic placement of Apostasioideae, drawing considerable attention from

orchid taxonomists and experts. The first species of *Apostasia* was found and initially classified under Orchidaceae in 1825 [6]. However, in 1833, Lindley advocated considering Apostasiaceae as a separate family, in juxtaposition to Orchidaceae [6]. Recent studies, based on morphological evidence, have suggested that Apostasioideae would be more appropriately considered a subfamily of Orchidaceae, standing apart from all other orchids lineages due to their unique characteristics: an incipient gynostemium and three stamens, which are considered ancient traits of the orchid lineage [7,8]. Despite these two genera exhibiting similar floral structures, previous studies argue that *Apostasia* is not even closely related to *Neuwiedia* [9] and is believed to have a closer relationship with the Cypripedioideae based on the staminode character [10]. This distinction has prompted suggestions for creating a separate family exclusively for *Neuwiedia* [11]. Furthermore, Rao strongly suggested, based on floral vasculature, that the subtribe Cypripedilinae have evolved directly from Apostasiaceae [12]. In order to further investigate inter- and intrageneric relationships within Apostasioideae, beyond relying solely on morphological observations, sequencing chromosome-scale and complete plastid genomes have unveiled new insights. In molecular systematics, *A. wallichii* has more related taxa with *A. ramifera* and *A. shenzhenica* than *A. odorata* based on its complete plastome and 68 protein-coding genes [13,14], while *A. wallichii* is sister to *A. odorata* based on *matK*, *rbcL*, *psbA-trnH*, *trnL-F*, *trnS-G*, and the nuclear ITS region [15,16]. In terms of genome size, Jersáková research indicates that Apostasioideae, on average, possess the smallest genome size among Orchidaceae families, with *Apostasia* displaying a notably smaller genome compared to the non-overlapping genome sizes observed in *Neuwiedia* [17]. Within *Apostasia*, *A. fujianica* is sister to *A. shenzhenica*, but the genome size of this was the smallest among all previously reported *Apostasia* species [18]. Anyway, the taxonomy of Apostasioids remains inconclusive due to limited availability of plant material and an inadequate understanding of phenotypic variation, leading to poor taxonomic classification.

Genetic information has proven to be an effective approach to understanding evolutionary relationships and resolve phylogenetic issues, and the abundant genetic data in the chloroplast genome can be utilized for comparative analysis and research on species diversification [19,20]. It is noteworthy that a fascinating large inversion has been observed in the plastid of *Apostasia*, a feature not identified in other existing orchid plastid structures [21]. This discovery merits further investigation and exploration into the plastid structure of primitive orchids. In this study, we generated two newly complete plastomes of Apostasioideae species (*Apostasia fujianica* and *Neuwiedia malipoensis*) and conducted comparative genomic analysis, including plastid structure, sequence repeats, codon usage, and nucleotide variability, with the five previously published ones (*A. odorata*, *A. ramifera*, *A. shenzhenica*, *A. wallichii*, and *N. zollingeri* var. *singapureana*). Additionally, we constructed six phylogenetic trees to illustrate the relationship of these seven species within Apostasioideae. Overall, our results provide valuable genetic resource for the further phylogenetic study of Apostasioideae species.

2. Materials and Methods

2.1. Plant Material Collection, DNA Extraction, and Sequencing

Fresh leaf samples of *A. fujianica* and *N. malipoensis* were frozen in liquid nitrogen and stored in a −80 °C refrigerator at Fujian Agriculture and Forestry University, Fuzhou, China. Then, total DNA extraction was carried out using a plant total genomic DNA kit (VazymeBiotech, Nanjing, China). Subsequently, a 350 bp paired-end library was prepared for sequencing utilizing the BGISEQ platform (Shenzhen, China). SOAPnuke 1.5.6 (https://github.com/BGIflexlab/SOAPnuke, accessed on 10 September 2023) was employed to eliminate low-quality bases (the bases with a quality value Q $\leq$ 20 account for more than 10% of the entire read, and the proportion of N-containing bases is greater than 1%) and adaptor sequences from the raw data to obtain clean reads, with the following parameters: -n 0.01, - l20, -q 0.1, -Q 2, -M 2, and -A 0.5.

2.2. Plastome Assembly and Annotation

The complete plastid genomes were assembled using GetOrganelle with default parameters (number of iterations: 15; Kmer: 21, 45, 65, 85, and 105; genome type: embplant_pt) [22]. Gene annotation was preliminary performed by using PGA software (https://github.com/quxiaojian/PGA, accessed on 12 September 2023) (-i 1000, -p 40, and -q 0.5,2) [23] with the plastomes of *A. wallichii* and *N. zollingeri* var. *singapureana* as references, and then manually examined through Geneious Prime v2023.2.1 [24]. After comparison with the other homologous genes, if a gene contained multiple stop codons or its sequence similarity was less than one-third of the reference gene, it was classified as a pseudogene. If the gene similarity was less than 50%, it was considered lost. Then, we checked the annotated genome using OGDRAW v1.3.1 [25] to identify any annotation issues. We continued to revise the annotation until no ERROR occurred in our annotation on the website, ensuring the quality and completeness of our annotation. Finally, the circular plastid genome maps were visualized using OGDRAW v1.3.1 [25].

2.3. Genome Comparison and Analysis

The sequences of *A. odorata* (KM244734), *A. ramifera* (MT864006), *A. shenzhenica* (MK370661), *A.wallichii* (LC199394), and *N. zollingeri* var. *singapureana* (LC199503) were included in the comparative plastid genome analysis. The mVISTA program (http://genome.lbl.gov/vista/mvista/instructions.shtml, accessed on 26 October 2023) was employed to compare seven species' plastome genomes with the sequence of *A. odorata* as a reference in the LAGAN model. In addition, we employed Mauve [26] to detect the rearrangements among different Apostasioideae plastomes. To better analyze the expansion/contraction events of the IR region, the boundaries between LSC/IR/SSC regions of all seven species' plastomes were compared and drawn using an online application CPJSdraw v1.0.0 [27].

2.4. Repeat Sequences and Codon Usage

Long sequence repeats (LSRs) were detected using REPuter (https://bibiserv.cebitec.uni-bielefeld.de/reputer, accessed on 27 October 2023), which identified four types of repeats: forward (F), palindrome (P), reverse (R), and complement (C). Parameters were set as follows: the maximum computed repeats (50 bp), the minimum repeat size (20 bp), and the hamming distance (3).

In the analysis of codon usage, we utilized codonW v1.4.4 (http://codonw.sourceforge.net/, accessed on 29 October 2023) to analyze relative synonymous codon use (RSCU) for each Apostasioideae species. And outcomes were visualized using Genenpioneer biotechnologies cloud platform (http://cloud.genepioneer.com, accessed on 29 October 2023).

2.5. Divergence Analyses and Phylogeny

Nucleotide variability (Pi) for the seven Apostasioideae plastomes and 68 protein-coding genes was computed using DnaSP 6 [28]. The analysis employed a window length of 100 sites and a step size of 25 sites, excluding sites with gaps. To construct the phylogenetic tree, we utilized protein-coding sequences from a total of 40 species. Among these, only *A. fujianica* and *N. malipoensis* were newly sequenced by us. The remaining 38 species are available at GeneBank: 34 from 5 subfamilies within the Orchidaceae family, and 4 (*I. cedreti*, *I. dichotoma*, *L. radiata*, and *L. aurea*) from outside this family, serving as outgroup species. The relevant accession numbers from NCBI are provided in Supplementary Table S3. We used PhyloSuite v1.2.2 [29] to extract and concatenate 68 protein-coding genes and each sequence underwent alignment using MAFFT-v7.409 [30] and subsequent trimming via trimAL v1.4 [31]. And then, we reconstructed a phylogenetic tree through the maximum likelihood, maximum parsimony, and Bayesian inference analysis, following the methodologies detailed in our previous study [32]. In addition, we selected the chloroplast genes *matK*, *psaB*, *rbcL*, and *ycf2* and genes identified through the Pi analysis to construct ML phylogenetic trees for establishing the subfamily-level classification system of Orchidaceae using PhyloSuite v1.2.2 [29].

3. Results

3.1. Plastid Genome Features

The genome sizes of *A. fujianica* and *N. malipoensis* were determined to be 153,179 bp and 163,193 bp, respectively (Figure 1), accompanied by corresponding GC contents of 35.9% and 35.6% (Table 1). Notably, the plastid lengths of two *Neuwiedia* species surpassed 160,000 bp, while those of all five *Apostasia* species consistently remained below this figure. Moreover, both plastomes displayed a typical quadripartite structure. For *A. fujianica*, the IR regions occupied 27,510 bp, constituting 17.96% of its total length. Meanwhile, the IR region length of *N. malipoensis* was 27,076 bp, accounting for 16.59%, showing similarity to that of *N. zollingeri* var. *singapureana* (26,959 bp, 16.75%). The SSC region of *A. fujianica* was the second smallest among the seven Apostasioideae genomes, measuring 11,981 bp, while in *N. malipoensis*, it extended to 18,487 bp. The LSC region of *A. fujianica* (86,178 bp) was similar to that of *A. shenzhenica* (86,167 bp). However, the LSC region of *N. malipoensis* spanned 90,554 bp, ranking as the longest among the seven genomes.

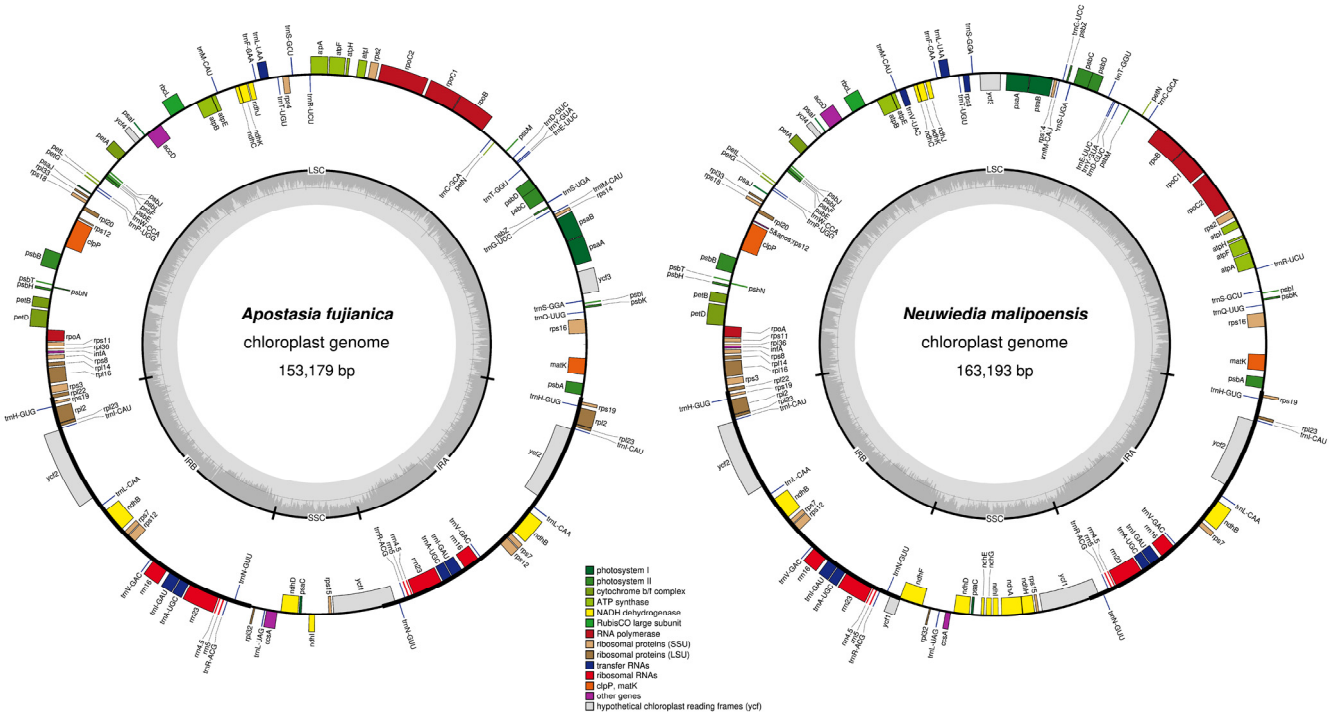

Figure 1. Plastome annotation maps of *Apostasia fujianica* and *Neuwiedia malipoensis*. The darker gray portion inside the inner circle represents the GC content, while the lighter gray portion represents the AT content. The inner circle is divided into four sections: the LSC region, IRa region, IRb region, and SSC region.

Table 1. Characteristics of complete plastomes of seven Apostasioideae species.

Species Name	Size (bp)	GC Content (%)	LSC Size in bp (%)	IR Size in bp (%)	SSC Size in bp (%)	Total Number of Genes	Protein-Encoding Genes	tRNA	rRNA	Number of *ndh* Fragments
A. odorata	159,285	35.7	86,288 (54.17)	27,116 (17.02)	18,765 (11.79)	133	86	38	8	11
A. ramifera	157,518	35.8	86,353 (54.82)	27,360 (17.37)	16,445 (10.44)	134	78	38	8	9
A. shenzhenica	153,164	35.9	86,167 (56.26)	27,510 (17.96)	11,977 (7.82)	130	77	40	8	6
A. wallichii	156,126	36.1	83,035 (53.18)	26,452 (16.94)	20,187 (12.94)	135	71	39	8	11
A. fujianica	153,179	35.9	86,178 (56.26)	27,510 (17.96)	11,981 (7.82)	123	74	35	8	6

Table 1. *Cont.*

Species Name	Size (bp)	GC Content (%)	LSC Size in bp (%)	IR Size in bp (%)	SSC Size in bp (%)	Total Number of Genes	Protein-Encoding Genes	tRNA	rRNA	Number of *ndh* Fragments
N. zollingeri var. *singapureana*	161,068	36.0	89,060 (55.29)	26,959 (16.75)	18,058 (11.21)	135	71	39	8	11
N. malipoensis	163,193	35.6	90,554 (55.49)	27,076 (16.59)	18,487 (11.33)	129	74	37	8	11

The plastid genomes of *A. fujianica* and *N. malipoensis* comprised 123–129 genes, including 74 protein-coding genes, 35–37 transfer RNA (tRNA), and 8 ribosomal RNA (rRNA). Among them, it was evident that most Apostasioideae species possessed 11 pseudogenes (*ndh A*/*B*/*C*/*D*/*E*/*F*/*G*/*H*/*I*/*J*/*K*). However, *A. fujianica* and *A. shenzhenica* presented the fewest *ndh* genes, lacking the *ndh A*/*E*/*F*/*G*/*H* gene and *A. ramifera* lost the *ndh A*/*I* gene.

The IR boundary map revealed stable LSC/IRb (JLB) and LSC/IRa (JLA) boundaries among the seven Apostasioideae plastomes (Figure 2), characterized by the surrounding distribution of the *rps19*, *psbA*, and *rpl22* genes. However, great variations were observed among these Apostasioideae species in the locations of the SSC/IRb (JSB) and SSC/IRa (JSA) boundaries. The JSB boundary of most species remained between the *ycf1* and *ndhF* genes, but that of *A.fujianica* was positioned between the *ycf1* and *rpl32* genes, resembling the arrangement in *A. shenzhenica*. Furthermore, the gene *ycf1* straddled the SSC and IRa region among these species.

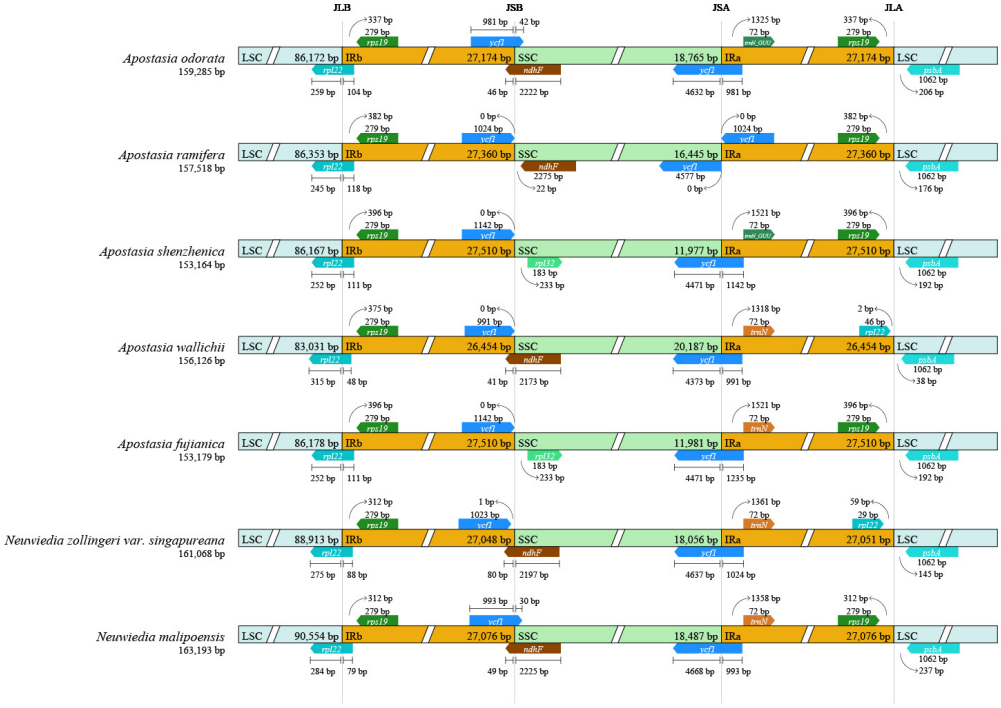

Figure 2. Comparison of the boundaries between LSC/SSC and IR regions in the seven Apostasioideae species.

3.2. Codon Preference Analysis

Codons play a crucial role in transferring genetic information from mRNA to proteins, encompassing 61 types responsible for coding 20 distinct amino acids. Within the plastid genomes of *A. fujianica* and *N. malipoensis*, the protein-coding genes (PCGs) contained 18,171 and 18,010 codons, respectively (Supplementary Table S1). Across selected Apostasioideae species, PCGs were encoded by a range from 16,539 (*A. ramifera*) to 19,950 (*A. odorata*) codons. Among them, leucine (Leu) emerged as the most frequently occurring amino acid, totaling 12,824 instances across all seven plastomes, closely followed by isoleucine (Ile) appearing 10,774 times. Conversely, cysteine (Cys) was the least utilized amino acid, with

only 1460 occurrences. The relative synonymous codon usage (RSCU) values of the seven species are depicted in Figure 3. The results highlighted AGA and UUA as the codons with higher usage bias, with average values of 1.93 and 1.91, respectively. And the RSCU values of UGG encoding tryptophan (Trp) and AUG encoding methionine (Met) were both determined to be 1.

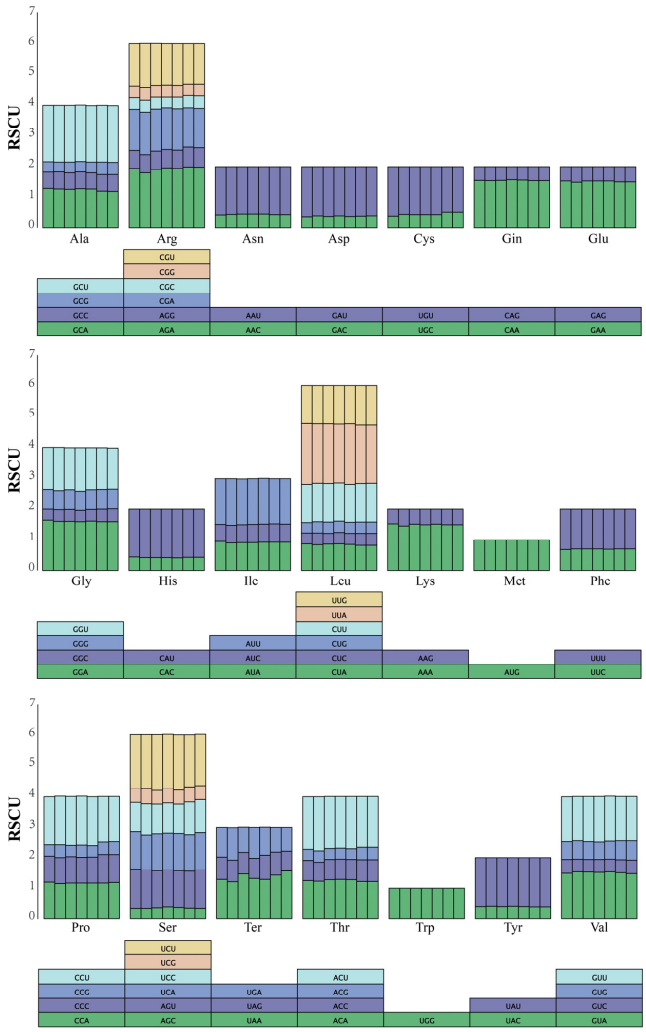

Figure 3. Relative synonymous codon usage value in all protein-coding genes of the seven plastomes of Apostasioideae species. The histogram above each amino acid is arranged in the order of *A. odorata*, *A. ramifera*, *A. shenzhenica*, *A. wallichii*, *A. fujianica*, *N. zollingeri* var. *singapureanam*, and *N. malipoensis*.

3.3. Plastome Sequence Divergence

The plastid genome sequence of *A. odorata* served as the reference to compare the genomic sequences of six Apostasioideae plastid genomes using mVISTA analysis. As depicted in Figures 4 and 5, the result showed substantial differences between the two *Neuwiedia* species and the remaining five *Apostasia* species. Notably, a reversal in the gene order was observed within the LSC region of *Apostasia* species, specifically between 10k and 47k bp, signifying distinct variations. Additionally, we identified two small segments that underwent inversion: one present in all *Apostasia* species (except *A.wallichii*), approximately at 58k–59k bp, and another occurring specifically at 118k–119k bp, found exclusively in the plastid genomes of *A. shenzhenica* and *A. fujianica*. Interestingly, within the 118k–119k bp range, *A. odorata* and *A.wallichii* did not undergo rearrangement, whereas in *A. ramifera*, the gene sequence was completely lost. Moreover, the IR region exhibited higher conservation compared to the LSC and SSC regions.

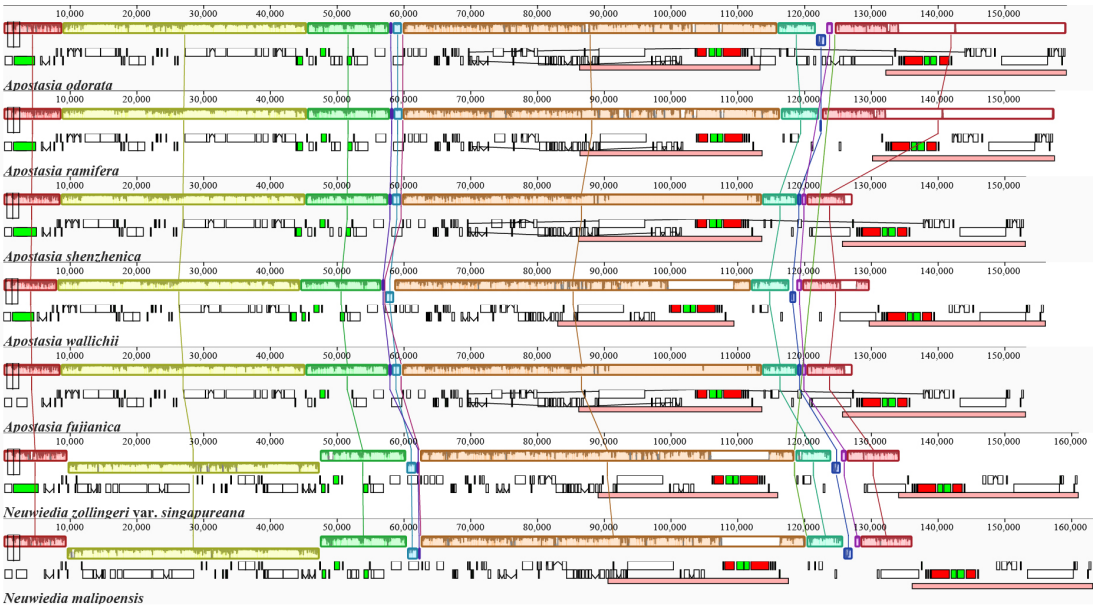

Figure 4. Synteny analysis of the seven Apostasioideae plastomes sequences. The plastid genome of *A. odorata* serves as the reference sequence.

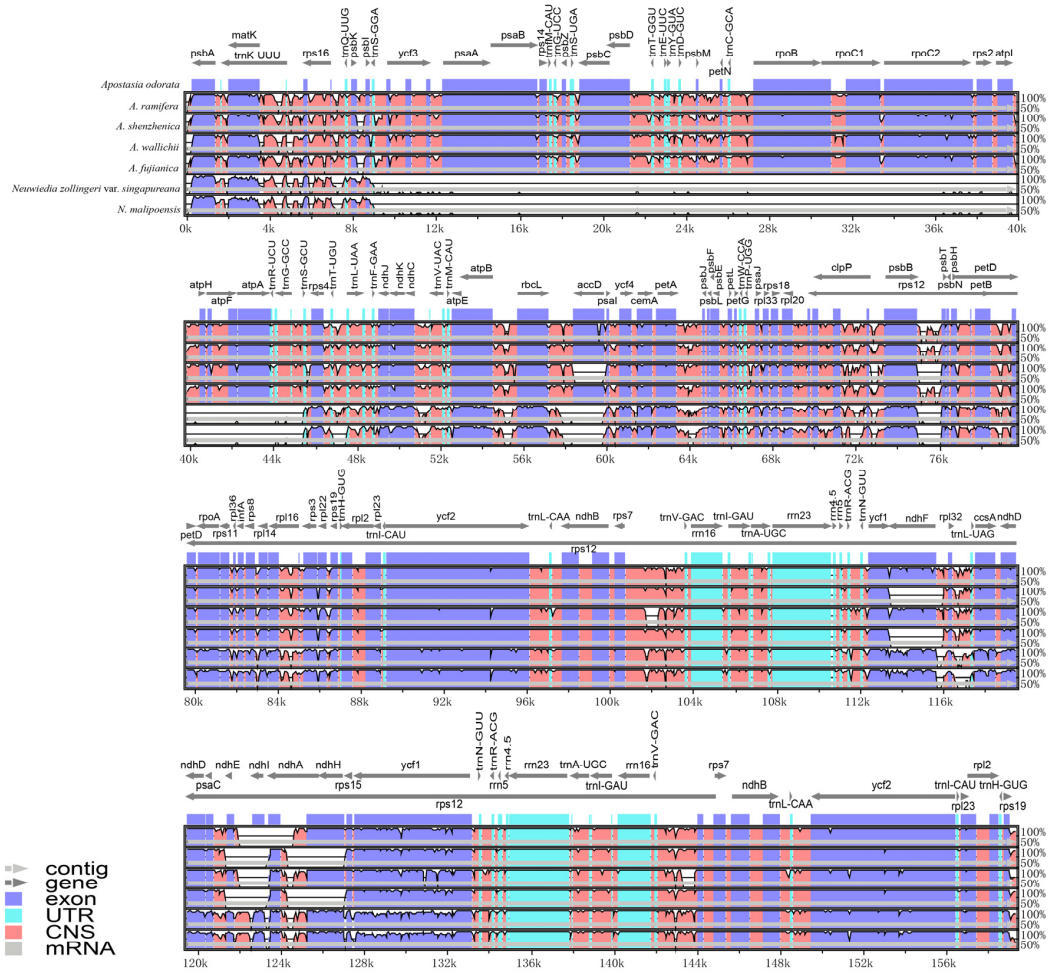

Figure 5. mVISTA analysis of the seven plastomes of Apostasioideae. The plastome of *A. odorata* was used as a reference.

3.4. Repeat Analysis and Mutation Hotspot Investigation

Among these 7 Apostasioideae plastid genomes, a total of 334 long repeats were identified and classified into complement (C, 12), forward (F, 124), palindrome (P, 146), and reverse (R, 52) types (Figure 6). The long-repeat count varied across the species: 50 in *A. shenzhenica*, 49 in *A. odorata*, *A. ramifera*, *A. fujianica*, and *N. malipoensis*, 47 in *N. zollingeri* var. *singapureana*, and 41 in *A. wallichii*. Additionally, four types of repeats were predominantly observed within the 30–39 bp range. Neither *A. ramifera* nor *A. wallichii* showed any complement repeats. In the 20–29 bp range, *A. odorata* and *A. ramifera* displayed a higher count of long repeats. In the 30–39 bp range, *A. shenzhenica*, *A. fujianica*, and *N. malipoensis* exhibited more long repeats. In the 40+ bp range, *A. wallichii* showed the highest count of long repeats. The relevant information is provided in Supplementary Table S2.

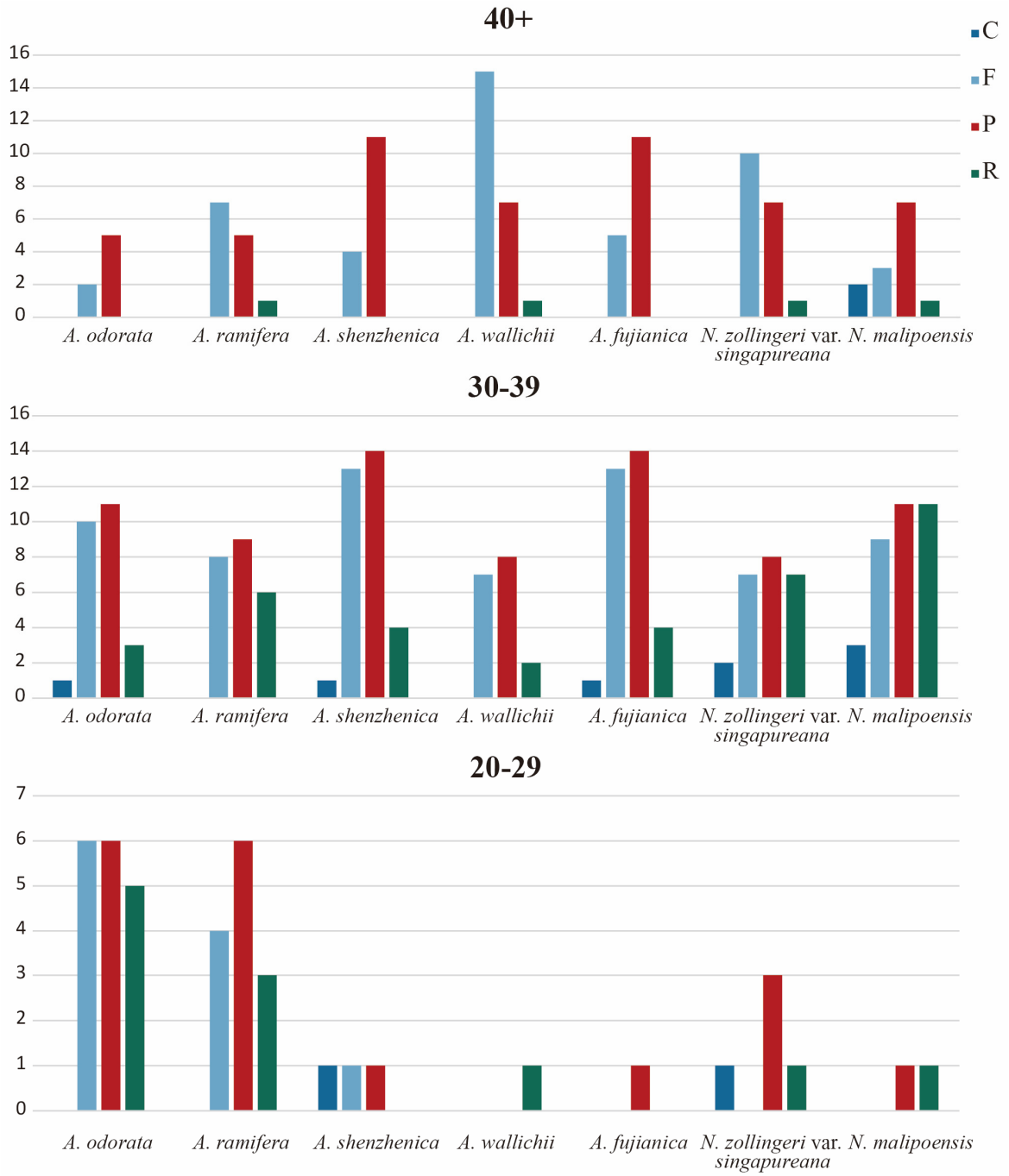

Figure 6. Analysis of long repeated sequences of the seven plastomes of Apostasioideae.

To identify highly mutated hotspots within Apostasioideae plastid genomes, nucleotide diversity (Pi) was calculated using DnaSP6 (Figure 7A). The Pi values ranged from 0 to 0.36571 across the seven plastomes. At the cutoff point Pi > 0.3, we selected five mutational hotspots (*clpP* > *rpoC2* > *atpH* > *ndhK* > *rps4*) as candidate barcodes. Furthermore, protein-coding genes underwent nucleotide diversity analysis (Figure 7B) at the cutoff point of Pi > 0.05, revealing three coding sequences (*ccsA*, *rpl32,* and *ycf1*) with notable nucleotide diversity, thus rendering them suitable candidates for phylogenetic analysis.

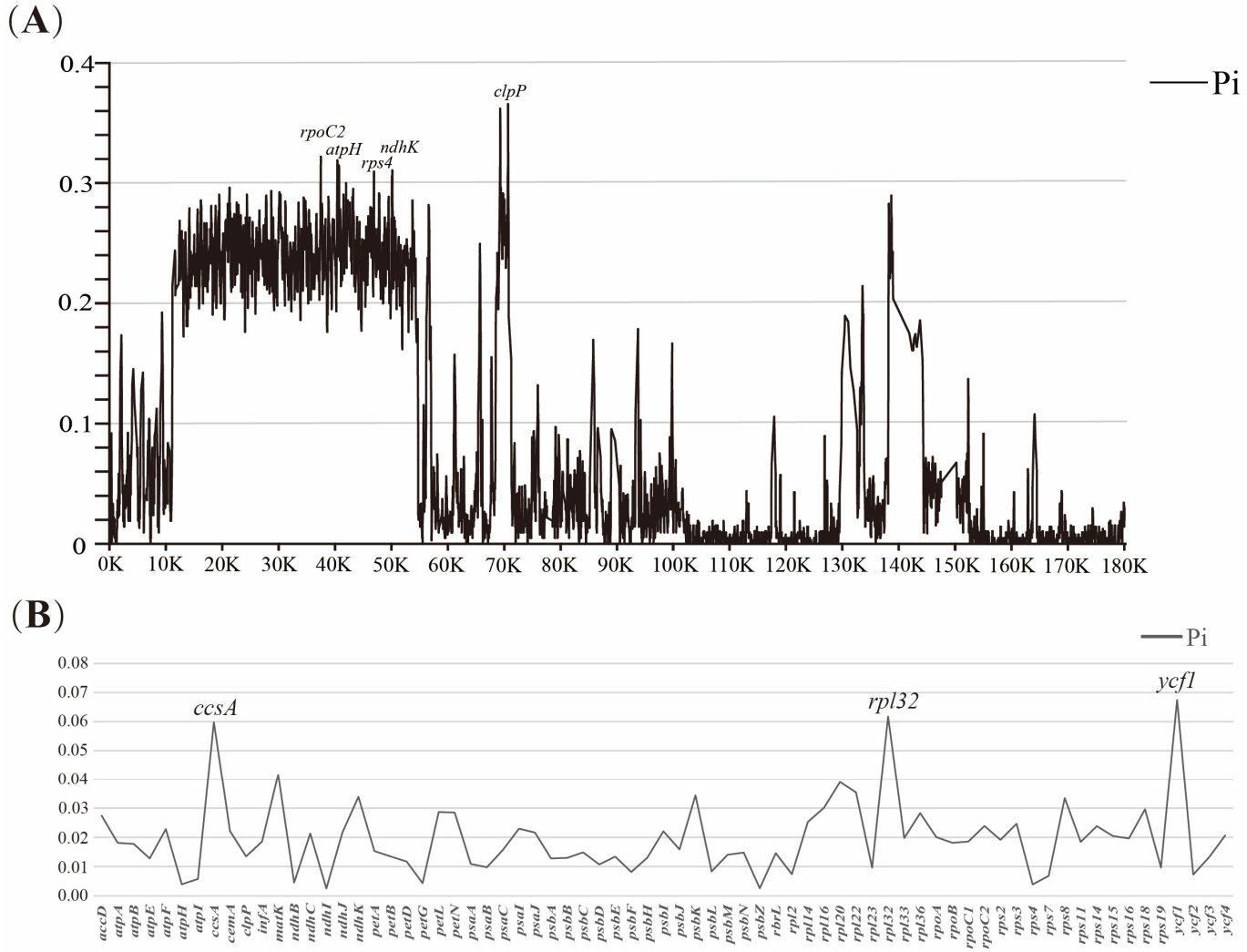

Figure 7. Sliding window analysis of the seven Apostasioideae plastomes. (**A**) The nucleotide diversity (Pi) of the complete plastomes and five mutation hotspot regions (Pi > 0.3) were annotated. (**B**) The Pi value of 68 protein-coding sequences showing three mutation hotspot regions (Pi > 0.05).

3.5. Phylogenetic Analysis

To investigate the phylogenetic position of Apostasioideae in the Orchidaceae family and the relationship among the Apostasioideae species, a comprehensive phylogenetic analysis was performed. This analysis utilized ML, MP, and BI methods employing 68 protein-coding genes of 36 Orchidaceae species along with 4 chosen outgroup species (*Iris cedreti*, *I. dichotoma*, *Lycoris radiata*, and *L. aurea*) (Figure 8). Our phylogenetic tree indicated that the subfamily Apostasioideae (BS = 100; PP = 1.00) diverged first, standing as a sister group to the remaining orchid taxa. Following this, Vanilloideae (BS = 100; PP = 1.00) diverged, which is sister to a strongly supported group (BS_{ML} = 95%, BS_{MP} = 100%, and PP = 1.00) comprising Cypripedioideae (BS = 100; PP = 1.00), Orchidoideae (BS = 100; PP = 1.00), and Epidendroideae (BS = 100; PP = 1.00). Specifically, *Neuwiedia* was robustly

supported as a monophyletic group (BS = 100; PP = 1.00) and positioned as a sister to *Apostasia*. Within *Apostasia*, five species were classified into two clades. *A. odorata* was supported as the first clade, while *A. ramifera*, *A. wallichii*, *A. shenzhenica*, and *A. fujianica* constituted the second clade with the following relationships: ((*A. ramifera* and *A. wallichii*) (*A. shenzhenica* and *A. fujianica*)). All branch nodes in this phylogenetic tree were strongly supported by the ML, MP, and BI analysis.

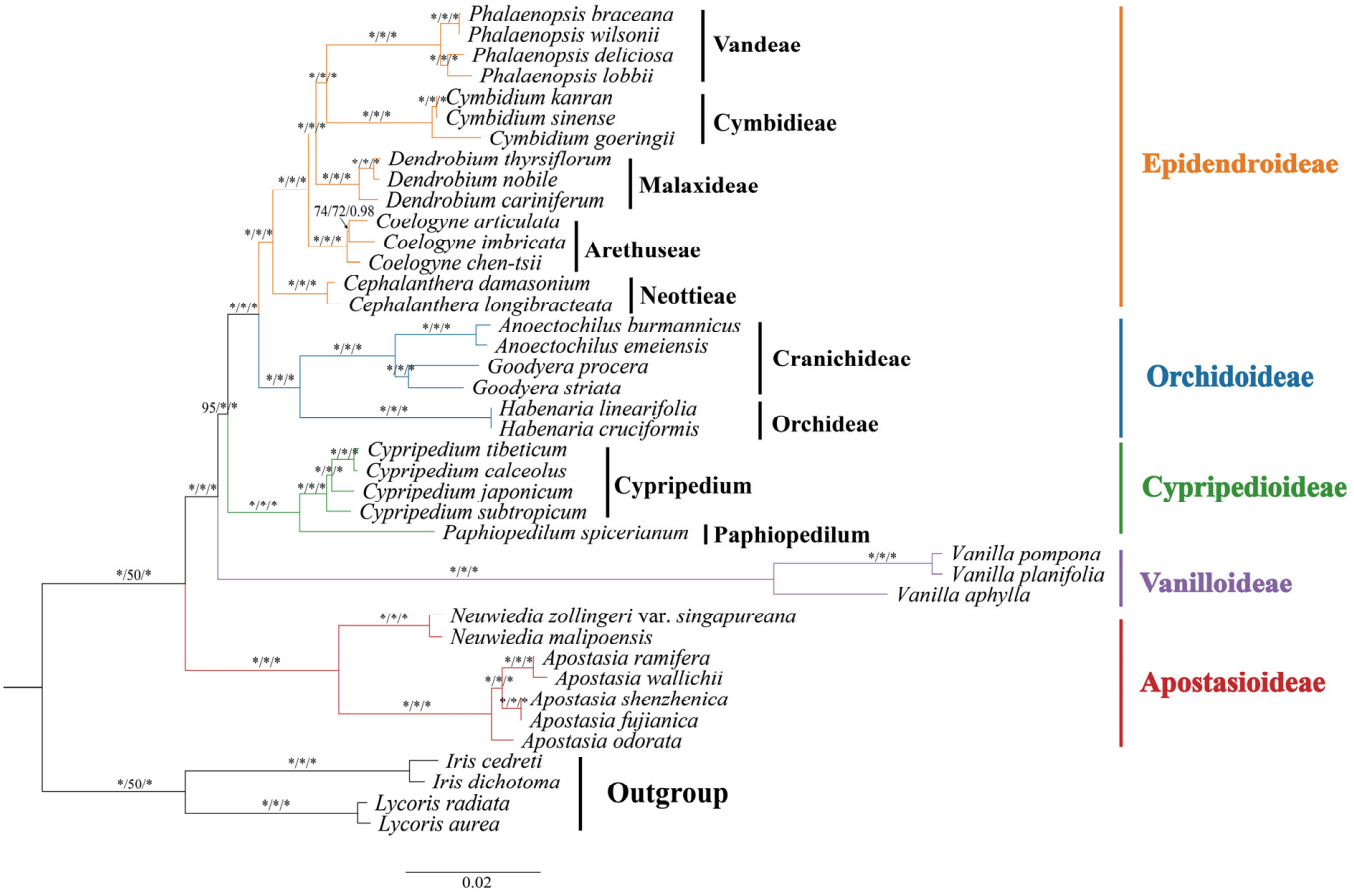

Figure 8. A phylogenetic tree constructed using the ML, MP, and BI methods, based on 36 different Orchidaceae species and 4 outgroup species. The BS_{ML} is on the left, the BS_{MP} is in the middle, and the PP is on the right. "*" represents 100% bootstrap or 1.00 probability.

Additionally, we selected the four genes *matK*, *pasB*, *rbcL*, and *ycf2* for the subfamily-level systematic reconstruction of Orchidaceae. And based on the Pi analysis results, we selected eight genes from hypervariable regions, including *rpoC*, *atpH*, *rps4*, *ndhK*, *clpP*, *ccsA*, *rpl32*, and *ycf1*, to construct an ML phylogenetic tree (Figure 9). The majority of bootstrap values supporting the Apostasioideae lineage in these five phylogenetic trees were above 70%, and they also supported the placement of Apostasioideae at the base of the Orchidaceae family, indicating that it represents the earliest diverging lineage. All results support the division of *Apostasia* into three distinct lineages: *A. odorata* forming the first lineage, *A. shenzhenica* and *A. fujianica* forming the second lineage, and *A. ramifera* and *A. wallichii* being supported as the third lineage.

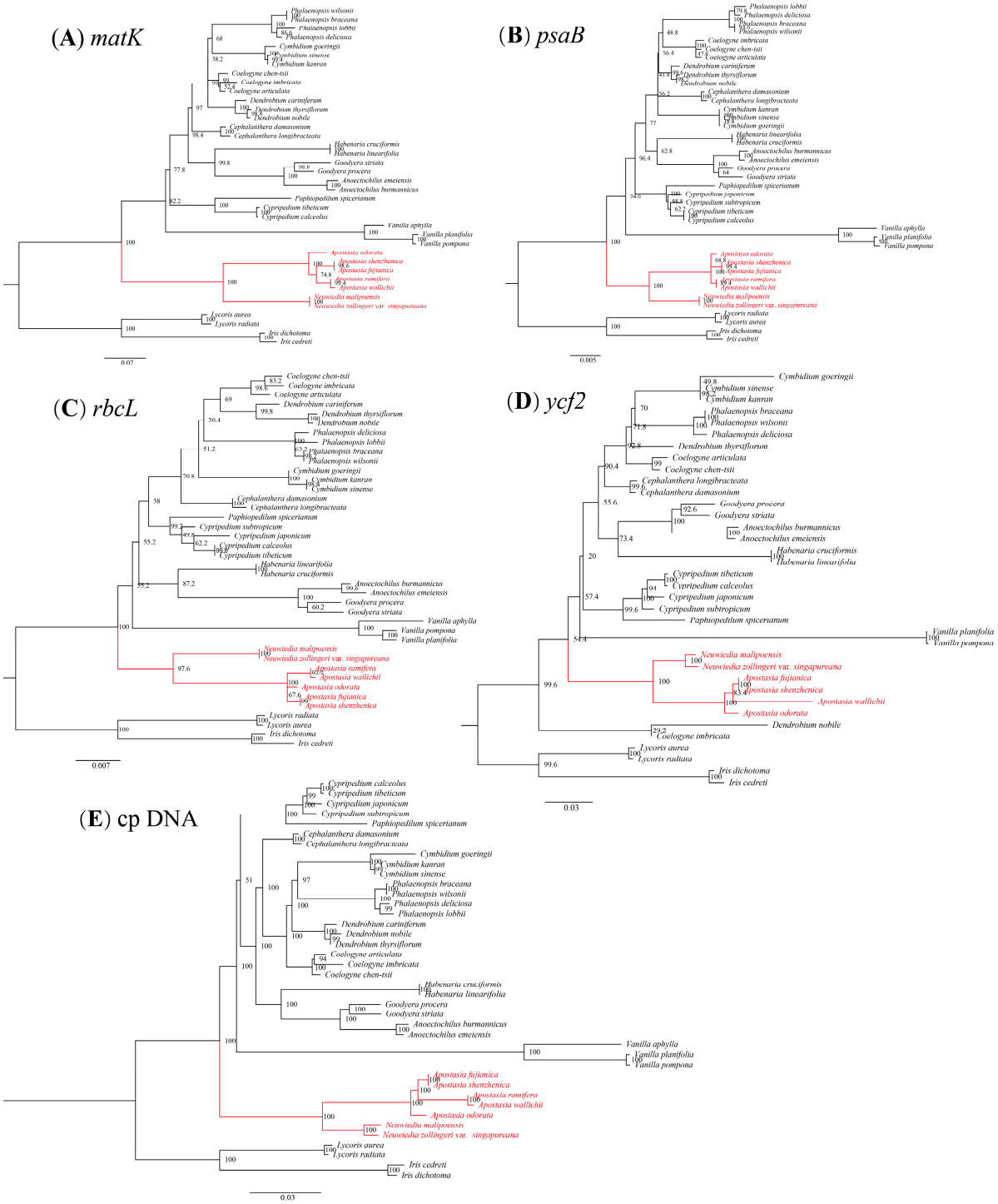

Figure 9. Phylogenetic tree constructed using ML method from plastid data, including (**A**) *matK*, (**B**) *psaB*, (**C**) *rbcL*, (**D**) *ycf2*, and (**E**) eight PCGs from Pi analysis (*rpoC*, *atpH*, *rps4*, *ndhK*, *clpP*, *ccsA*, *rpl32*, and *ycf1*). Position of Apostasioideae is highlighted in red.

4. Discussion

4.1. The Plastome Characteristics and Structural Rearrangement

The subfamily Apostasioideae, the most primitive group of the Orchidaceae, contains only two genera, *Apostasia* and *Neuwiedia*, with approximately 20 species [33–35]. However, only five Apostasioideae plastid genomes are available in public online databases, impeding our comprehensive understanding of orchid evolution within the basal lineages of the

orchid family. In our study, we employed next-generation sequencing technology to sequence the plastomes of *A. fujianica* and *N. malipoensis*. And our results align with the size reported for previously studied species. Among the seven Apostasioideae species, we observed that the sizes of *A. fujianica* (153,179 bp) and *A. shenzhenica* (153,164 bp) were very close, both falling below the 155k bp threshold. In contrast, the other three *Apostasia* species exceeded 155k bp, with *A. odorata* boasting the largest size at 159,285 bp. Notably, *A. fujianica* and *A. shenzhenica* exhibited striking similarities in LSC, SSC, and IR region length and the number of CDSs, consistent with their close phylogenetic relationship. Additionally, our findings revealed that *Neuwiedia* species consistently surpassed *Apostasia* in genome size, averaging more than 160k bp, while *Apostasia* remained below this threshold. Furthermore, our newly sequenced *N. malipoensis* exhibited the largest genome size (163,193 bp) among the published Apostasioideae species.

The *ndh* genes, as characterized in earlier studies, exhibit close resemblances to genes found in cyanobacteria, corroborating the endosymbiotic theory regarding chloroplast evolution [36]. These genes, designated as *ndh A-K*, are integral components of the plastid genome in higher plants, responsible for encoding proteins homologous to complex I subunits [37]. These proteins play a pivotal role in optimizing photosynthesis under diverse stress conditions [38]. In the orchid family, it is common for species to have experienced loss or pseudogenization of these *ndh* genes. Especially in epiphytic orchids, like *Dendrobium* [39], the loss is particularly severe. The reasons behind this loss could potentially be linked to their epiphytic lifestyle. And according to phylogenetic classifications, there has been an independent loss of *ndh* genes across all five subfamilies, while Apostasioideae exhibited a relatively low frequency [19,20]. In our study, a peculiar observation was made regarding the *ndh* genes in Apostasioideae species. Among the Apostasioideae species analyzed, four species—*A. odorata*, *A. wallichii*, *N. zollingeri* var. *singapureana*, and *N. malipoensis*—were found to retain all of the *ndh* genes. However, a distinctive pattern emerged among the remaining three species—*A. ramifera*, *A. shenzhenica*, and *A. fujianica*—where losses were identified in two (*ndh A*/*I*), five (*ndh A*/*E*/*F*/*G*/*H*), and five (*ndh A*/*E*/*F*/*G*/*H*) *ndh* genes, respectively. The intriguing aspect here is that despite belonging to terrestrial habitats, these Apostasioideae species also exhibited loss or pseudogenization of *ndh* genes. While some researchers have previously associated the loss of *ndh* genes with epiphytic habits [19], our findings challenge this notion as the Apostasioideae, being terrestrial plants, display similar gene losses. This situation prompts the need for further exploration of the underlying reasons for *ndh* gene loss in Apostasioideae.

Like other angiosperms, plastomes in most orchid plants exhibit the characteristic division into the SSC, LSC, and IR regions (a typical quadripartite structure) [40]. Expansion or contraction in the IR region are common in plastomes during land plant evolution [41], significantly influencing variations in plastid genome sizes [42]. However, some mycoheterotrophic orchids show the expansion of their LSC region rather than their IR region [19]. In our study, we noticed a slight difference in the boundary between the LSC and IR regions. At the junction of JLB, the *rpl22* gene was found in seven species. Regarding JLA, all species except *A. wallichii* and *N. zollingeri* var. *singapureana* (between *rpl22* and *psbA* gene) were positioned between the *rps19* and *psbA* genes. However, variations in JSB could be attributed to the absence of *ndhF* in *A. shenzhenica* and *A. fujianica*.

In general, it is widely acknowledged that plastid genomic rearrangements are common in monocotyledonous plants. This phenomenon has been recently observed in orchid plastids, encompassing *Cypripedium* [43], *Pogonia* [44], and *Goodyera* [45]. Furthermore, previous research indicates that the probability of plastid rearrangement in orchids is highest in the SSC region (64.4%), followed by the LSC region (32.7%), and lastly the IR region (2.9%) [19,46]. Mauve analyses were conducted in this study, revealing a collinear analysis of seven species. And a notable feature distinguishing *Neuwiedia* from *Apostasia* was observed, as shown in Figures 4 and 5. We identified three distinctive structural inversions in *Apostasia* species. Firstly, there is large segment gene rearrangement in the LSC region (10k-47k bp) of *Apostasia* genus, which is a shared *Apostasia*-specific rearrangement

(*ycf3–trnS-GCU*), consistent with previous research findings [44]. Moreover, two small segment rearrangements have been newly identified in the LSC region (58k–59k bp) and the SSC region (118k–119k bp). Within the 58–59k bp region (the *accD* gene) of *Apostasia* plastids, excluding *A. wallichii*, a distinct rearrangement is shared. Another independent rearrangement (118k–119k bp, *ndhI*) was observed in *Apostasia* plastids, with structural inversion observed solely in *A. shenzhenica* and *A. fujianica*, and even absent in *A. ramifera*. This segment sequence may encode a distinct genetic signature for *A. shenzhenica* and *A. fujianica*. Hence, minor rearrangements in *Apostasia* likely represent later intragenus rearrangements triggered by incomplete or lost genes, whereas the large-scale rearrangement may denote a characteristic feature of the ancestral orchid plastid.

4.2. Polymorphic Loci for Molecular Markers

Currently, plastid gene sequences are extensively utilized by plant molecular systematics and DNA barcoding techniques [47]. The mutations in the plastomes are not evenly distributed across the sequence. They often occur in hotspot regions, representing ideal markers for developing DNA barcodes [48]. There has been a lot of research in orchids focused on DNA barcoding development, including *rbcL*+ITS and *matK*+ITS (*Oberonia*) [49]; *trnT-trnL*, *rpl32-trnL*, *clpP-psbB*, *trnL* intron, and *rps16-trnQ* (*Dendrobium*) [39]; and *trnG-trnR*, *trnR-atpA*, *trnP-psaJ*, *rpl32-infA*, and *rps15-ycf1* (*Cranichidinae*) [50]. In our study, the sliding window analysis identified four highly variable regions, while the Pi analysis of protein-coding genes revealed three highly variable coding genes. These specific seven mutation regions could effectively function as DNA barcodes for distinguishing the Apostasioideae from the other four subfamilies. Repetitive sequences play an important role in the evolution of species by expanding genome size and influencing chromosomal recombination [51,52]. Here, we identified a total of 41–50 long repeats across seven species. The number of complement (5) and reverse (14) repeats in *N. malipoensis* are the highest among Apostasioideae species, while the forward (18) and palindrome (26) repeats in *A. fujianica* are similar to those in *A. shenzhenica*. Additionally, the quantity of long repeats varies among different genera of orchids. For instance, *Aerides* has 49–65 long repeats [53], *Trichoglottis* has 33–46 [54], and *Epidendrum* has 25–38 [55]. We believe these results could serve as valuable molecular resources for DNA marker development.

4.3. Phylogenetic Analysis

Apostasioideae comprises the genera *Apostasia* and *Neuwiedia*, and their position in the phylogenetic tree has been controversial [7]. Some previous studies suggested that there is a closer relationship between Apostasioideae and lower Asparagales, Liliales, or Haemadorales [7,56]. However, anatomical and DNA studies indicate an exclusive association of these two genera with the rest of the orchids [7,57]. Our phylogenetic tree based on CDS sequences strongly supports the monophyly of Apostasioideae and their sister-group relationship to the remaining orchids, consistent with previously reported results [56,58]. *N. zollingeri* var. *singapureana* and *N. malipoensis* formed a monophyletic group, and *Apostasia* was sister to *Neuwiedia*. Within the section *Apostasia*, our analyses support the following relationship: (*A.odorata* (*A. shenzhenica* and *A. fujianica*) (*A. ramifera* and *A. wallichii*)). However, our results contradict the conclusion of the phylogenetic tree of Apostasioideae based on plastid DNA and nuclear ribosomal ITS, which suggests that the five *Apostasia* species are divided into two groups: *A. wallichii* and *A. odorata* form a monophyletic group sister to *A. ramifera*, *A. fujianica*, and *A. shenzhenica*. Our results, based on the reconstruction of multiple phylogenetic trees using four core chloroplast genes and genes with high nucleotide diversity, consistently support our classification of *Apostasia* with high bootstrap values. Overall, this study has reconstructed their systematic evolutionary relationships and provides a more comprehensive understanding of the evolutionary relationships within the Apostasioideae.

5. Conclusions

This study is the first to sequence and assemble plastomes of *A. fujianica* and *N. malipoensis* and perform a comparison with the other five closely related species from Apostasioideae. Our findings show that *N. malipoensis* exhibits the largest genome size (163,193 bp) among the published Apostasioideae species so far. Additionally, we have discovered three structural rearrangements in the plastid genomes of *Apostasia*, located in the LSC region (two: *ycf3–trnS-GCU,* and accD) and the SSC region (one: *ndhI*). And *clpP*, *rps4*, *rpoC2*, *atpF*, and *ndhK* with high Pi values are recommended as available DNA barcodes of Apostasioideae. The phylogenetic tree reveals a close relationship between the genera *Apostasia* and *Neuwiedia*, and further confirms that *A. ramifera* is the most related taxa with *A. wallichii*, and *A. shenzhenica* is the most related taxa with *A. fujianica*. In summary, our findings contribute to the understanding of the phylogenetic status of Apostasioideae and provide valuable genetic data for future studies on Apostasioideae or other orchids.

Supplementary Materials: The following supporting information can be downloaded at: https://www.mdpi.com/article/10.3390/horticulturae10040383/s1, Table S1: Codon Preference of seven Apostasioideae species; Table S2: Repeated Analysis of seven Apostasioideae species; Table S3: Genbank accessions of 40 species.

Author Contributions: Q.Z. finalized the manuscript and integrated all other authors' comments; D.-K.L. provided the data; Y.W. and S.-J.K. analyzed the data; Z.-J.L. conceived the study idea, coordinated with all of the coauthors, and supervised the whole project. All authors have read and agreed to the published version of the manuscript.

Funding: This work was supported by the National Natural Science Foundation of China (KAy22014XA); the Technical Services for Introduction and Domestication of Orchids in Sanjiangkou Botanical Garden, Fuzhou (KH240047A); the Vanilla Genome Analysis and Functional Exploration of Key Genes (KFB23176A).

Data Availability Statement: Data are contained within the article and supplementary materials. The newly complete plastomes accession numbers: PP599181 (*Apostasia fujianica*) and PP601065 (*Neuwiedia malipoensis*).

Conflicts of Interest: The authors declare no conflicts of interest.

References

1. Scotland, R.W.; Wortley, A.H. How many species of seed plants are there? *Taxon* **2003**, *52*, 101–104. [CrossRef]
2. Christenhusz, M.J.M.; Byng, J.W. The number of known plants species in the world and its annual increase. *Phytotaxa* **2016**, *261*, 201–217. [CrossRef]
3. Givnish, T.J.; Spalink, D.; Ames, M.; Lyon, S.P.; Hunter, S.J.; Zuluaga, A.; Iles, W.J.; Clements, M.A.; Arroyo, M.T.; Leebens-Mack, J.; et al. Orchid phylogenomics and multiple drivers of their extraordinary diversification. *Proc. R. Soc. B Biol. Sci.* **2015**, *282*, 20151553. [CrossRef]
4. Chen, X. Apostasioideae. *Flora China* **2017**, *25*, 20.
5. Rasmussen, H.N.; Rasmussen, F.N. Seedling mycorrhiza: A discussion of origin and evolution in Orchidaceae. *Bot. J. Linn. Soc.* **2014**, *175*, 313–327. [CrossRef]
6. de Vogel, E.F. Monograph of the tribe *Apostasieae* (Orchidaceae). *Blumea Biodivers. Evol. Biogeogr. Plants* **1969**, *17*, 313–350.
7. Stern, W.L.; Cheadle, V.I.; Thorsch, J. Apostasiads, systematic anatomy, and the origins of Orchidaceae. *Bot. J. Linn. Soc.* **1993**, *111*, 411–455. [CrossRef]
8. Suetsugu, K. A novel seed dispersal mode of *Apostasia nipponica* could provide some clues to the early evolution of the seed dispersal system in Orchidaceae. *Evol. Lett.* **2020**, *4*, 457–464. [CrossRef]
9. Garay, L.A. On the origin of the Orchidaceae, II. *J. Arnold Arbor.* **1972**, *53*, 202–215. [CrossRef]
10. Burns-Balogh, P.; Funk, V.A. A phylogenetic analysis of the Orchidaceae. *Smithson. Contrib. Bot.* **1986**, *61*, 1–79. [CrossRef]
11. Reveal, J.L.; Hoogland, R.D. Validation of three family names in the Magnoliophyta. *Bull. Muséum Natl. D'histoire Nat. Sect. B Adansonia* **1991**, *13*, 91–93.
12. Rao, V.S. The relationships of the Apostasiaceae on the basis of floral anatomy. *Bot. J. Linn. Soc.* **1974**, *68*, 319–327. [CrossRef]
13. Zheng, F.; Chen, J.B.; Liu, W.R.; Wang, M. The complete chloroplast genome of an endangered species *Apostasia ramifera* (Orchidaceae). *Mitochondrial DNA Part B* **2021**, *6*, 470–471. [CrossRef]
14. Li, Y.; Li, Z.; Hu, Q.; Zhai, J.; Liu, Z.; Wu, S. Complete plastid genome of *Apostasia shenzhenica* (Orchidaceae). *Mitochondrial DNA Part B* **2019**, *4*, 1388–1389. [CrossRef]

15. Kocyan, A.; Qiu, Y.L.; Endress, P.K.; Conti, E. A phylogenetic analysis of Apostasioideae (Orchidaceae) based on ITS, *trn*L–F and *mat*K sequences. *Plant Syst. Evol.* **2004**, *247*, 203–213. [CrossRef]
16. Yin, Y.Y.; Zhong, P.S.; Zhang, G.Q.; Chen, L.J.; Zeng, S.J.; Li, M.H.; Liu, Z.J. Morphological, genome-size and molecular analyses of *Apostasia fogangica* (Apostasioideae, Orchidaceae), a new species from China. *Phytotaxa* **2016**, *277*, 59–67. [CrossRef]
17. Jersáková, J.; Trávníček, P.; Kubátová, B.; Krejčíková, J.; Urfus, T.; Liu, Z.J.; Lamb, A.; Ponert, J.; Schulte, K.; Čurn, V.; et al. Genome size variation in Orchidaceae subfamily Apostasioideae: Filling the phylogenetic gap. *Bot. J. Linn. Soc.* **2013**, *172*, 95–105. [CrossRef]
18. Li, Y.; Ma, L.; Liu, D.; Zhao, X.; Zhang, D.; Ke, S.; Chen, G.Z.; Zheng, Q.; Liu, Z.J.; Lan, S. *Apostasia fujianica* (Apostasioideae, Orchidaceae), a new Chinese species: Evidence from morphological, genome size and molecular analyses. *Phytotaxa* **2023**, *583*, 277–284. [CrossRef]
19. Kim, Y.K.; Jo, S.; Cheon, S.H.; Joo, M.J.; Hong, J.R.; Kwak, M. Plastome evolution and phylogeny of Orchidaceae, with 24 new sequences. *Front. Plant Sci.* **2020**, *11*, 22. [CrossRef]
20. Kim, H.T.; Kim, J.S.; Moore, M.J.; Neubig, K.M.; Williams, N.H.; Whitten, W.M.; Kim, J.H. Seven new complete plastome sequences reveal rampant independent loss of the *ndh* gene family across orchids and associated instability of the inverted repeat/small single-copy region boundaries. *PLoS ONE* **2015**, *10*, e0142215. [CrossRef]
21. Niu, Z.; Pan, J.; Zhu, S.; Li, L.; Xue, Q.; Liu, W.; Ding, X. Comparative analysis of the complete plastomes of *Apostasia wallichii* and *Neuwiedia singapureana* (Apostasioideae) reveals different evolutionary dynamics of IR/SSC boundary among photosynthetic orchids. *Front. Plant Sci.* **2017**, *8*, 1713. [CrossRef]
22. Jin, J.J.; Yu, W.B.; Yang, J.B.; Song, Y.; DePamphilis, C.W.; Yi, T.S.; Li, D.Z. GetOrganelle: A fast and versatile toolkit for accurate de novo assembly of organelle genomes. *Genome Biol.* **2020**, *21*, 241. [CrossRef]
23. Qu, X.J.; Moore, M.J.; Li, D.Z.; Yi, T.S. PGA: A software package for rapid, accurate, and flexible batch annotation of plastomes. *Plant Methods* **2019**, *15*, 50. [CrossRef]
24. Kearse, M.; Moir, R.; Wilson, A.; Stones-Havas, S.; Cheung, M.; Sturrock, S.; Buxton, S.; Cooper, A.; Markowitz, S.; Duran, C.; et al. Geneious Basic: An integrated and extendable desktop software platform for the organization and analysis of sequence data. *Bioinformatics* **2012**, *28*, 1647–1649. [CrossRef]
25. Greiner, S.; Lehwark, P.; Bock, R. OrganellarGenomeDRAW (OGDRAW) version 1.3.1: Expanded toolkit for the graphical visualization of organellar genomes. *Nucleic Acids Res.* **2019**, *47*, W59–W64. [CrossRef]
26. Darling, A.C.E.; Mau, B.; Blattner, F.R.; Perna, N.T. Mauve: Multiple alignment of conserved genomic sequence with rearrangements. *Genome Res.* **2004**, *14*, 1394–1403. [CrossRef]
27. Li, H.; Guo, Q.; Xu, L.; Gao, H.; Liu, L.; Zhou, X. CPJSdraw: Analysis and visualization of junction sites of chloroplast genomes. *PeerJ* **2023**, *11*, e15326. [CrossRef]
28. Rozas, J.; Ferrer-Mata, A.; Sánchez-DelBarrio, J.C.; Guirao-Rico, S.; Librado, P.; Ramos-Onsins, S.E.; Sánchez-Gracia, A. DnaSP 6: DNA sequence polymorphism analysis of large data sets. *Mol. Biol. Evol.* **2017**, *34*, 3299–3302. [CrossRef]
29. Zhang, D.; Gao, F.; Jakovlić, I.; Zou, H.; Zhang, J.; Li, W.X.; Wang, G.T. PhyloSuite: An integrated and scalable desktop platform for streamlined molecular sequence data management and evolutionary phylogenetics studies. *Mol. Ecol. Resour.* **2020**, *20*, 348–355. [CrossRef]
30. Katoh, K.; Misawa, K.; Kuma, K.; Miyata, T. MAFFT: A novel method for rapid multiple sequence alignment based on fast Fourier transform. *Nucleic Acids Res.* **2002**, *30*, 3059–3066. [CrossRef]
31. Capella-Gutiérrez, S.; Silla-Martínez, J.M.; Gabaldón, T. trimAl: A tool for automated alignment trimming in large-scale phylogenetic analyses. *Bioinformatics* **2009**, *25*, 1972–1973. [CrossRef]
32. Li, Z.H.; Jiang, Y.; Ma, X.; Li, J.W.; Yang, J.B.; Wu, J.Y.; Jin, X.H. Plastid genome evolution in the subtribe Calypsoinae (Epidendroideae, Orchidaceae). *Genome Biol. Evol.* **2020**, *12*, 867–870. [CrossRef]
33. Garay, L.A. On the origin of the Orchidaceae. *Bot. Mus. Leafl. Harv. Univ.* **1960**, *19*, 57–96. [CrossRef]
34. Dahlgren, R.M.T.; Clifford, H.T.; Yeo, P.F. *The Families of the Monocotyledons: Structure, Evolution, and Taxonomy*; Springer Science & Business Media: Berlin/Heidelberg, Germany, 1984.
35. Suetsugu, K.; Matsubayashi, J. Evidence for mycorrhizal cheating in *Apostasia nipponica*, an early-diverging member of the Orchidaceae. *New Phytol.* **2021**, *229*, 2302–2310. [CrossRef]
36. Burrows, P.A.; Sazanov, L.A.; Svab, Z.; Maliga, P.; Nixon, P.J. Identification of a functional respiratory complex in chloroplasts through analysis of tobacco mutants containing disrupted plastid *ndh* genes. *EMBO J.* **1998**, *17*, 868–876. [CrossRef]
37. Matsubayashi, T.; Wakasugi, T.; Shinozaki, K.; Yamaguchi-Shinozaki, K.; Zaita, N.; Hidaka, T.; Meng, B.Y.; Ohto, C.; Tanaka, M.; Kato, A.; et al. Six chloroplast genes (*ndhA-F*) homologous to human mitochondrial genes encoding components of the respiratory chain NADH dehydrogenase are actively expressed: Determination of the splice sites in *ndhA* and *ndhB* pre-mRNAs. *Mol. Gen. Genet. MGG* **1987**, *210*, 385–393. [CrossRef]
38. Martín, M.; Sabater, B. Plastid *ndh* genes in plant evolution. *Plant Physiol. Biochem.* **2010**, *48*, 636–645. [CrossRef]
39. Niu, Z.; Zhu, S.; Pan, J.; Li, L.; Jing, S.; Ding, X. Comparative analysis of *Dendrobium* plastomes and utility of plastomic mutational hotspots. *Sci. Rep.* **2017**, *7*, 2073.
40. Perini, V.R.; Leles, B.; Furtado, C.; Prosdocimi, F. Complete chloroplast genome of the orchid *Cattleya crispata* (Orchidaceae: Laeliinae), a *Neotropical rupiculous* species. *Mitochondrial DNA Part A* **2016**, *27*, 4075–4077. [CrossRef]

41. He, S.; Yang, Y.; Li, Z.; Wang, X.; Guo, Y.; Wu, H. Comparative analysis of four Zantedeschia chloroplast genomes: Expansion and contraction of the IR region, phylogenetic analyses and SSR genetic diversity assessment. *PeerJ* **2020**, *8*, e9132. [CrossRef]
42. Dugas, D.V.; Hernandez, D.; Koenen, E.J.M.; Schwarz, E.; Straub, S.; Hughes, C.E.; Jansen, R.K.; Nageswara-Rao, M.; Staats, M.; Trujillo, J.T.; et al. Mimosoid legume plastome evolution: IR expansion, tandem repeat expansions and accelerated rate of evolution in *clpP*. *Sci. Rep.* **2015**, *5*, 16958. [CrossRef]
43. Lin, C.S.; Chen, J.J.; Huang, Y.T.; Chan, M.T.; Daniell, H.; Chang, W.J.; Hsu, C.T.; Liao, D.C.; Wu, F.H.; Lin, S.Y.; et al. The location and translocation of *ndh* genes of chloroplast origin in the Orchidaceae family. *Sci. Rep.* **2015**, *5*, 9040. [CrossRef]
44. Kim, Y.K.; Cheon, S.H.; Hong, J.R.; Kim, K.J. Evolutionary Patterns of the Chloroplast Genome in Vanilloid Orchids (Vanilloideae, Orchidaceae). *Int. J. Mol. Sci.* **2023**, *24*, 3808. [CrossRef]
45. Tu, X.D.; Liu, D.K.; Xu, S.W.; Zhou, C.Y.; Gao, X.Y.; Zeng, M.Y.; Zhang, S.; Chen, J.L.; Ma, L.; Zhou, Z.; et al. Plastid phylogenomics improves resolution of phylogenetic relationship in the *Cheirostylis* and *Goodyera* clades of Goodyerinae (Orchidoideae, Orchidaceae). *Mol. Phylogenetics Evol.* **2021**, *164*, 107269. [CrossRef]
46. Liu, D.K.; Zhou, C.Y.; Tu, X.D.; Zhao, Z.; Chen, J.L.; Gao, X.Y.; Xu, S.W.; Zeng, M.Y.; Ma, L.; Ahmad, S.; et al. Comparative and phylogenetic analysis of *Chiloschista* (Orchidaceae) species and DNA barcoding investigation based on plastid genomes. *BMC Genom.* **2023**, *24*, 749. [CrossRef]
47. Dong, W.; Liu, J.; Yu, J.; Wang, L.; Zhou, S. Highly variable chloroplast markers for evaluating plant phylogeny at low taxonomic levels and for DNA barcoding. *PLoS ONE* **2012**, *7*, e35071. [CrossRef]
48. Jiao, L.; Lu, Y.; He, T.; Li, J.; Yin, Y. A strategy for developing high-resolution DNA barcodes for species discrimination of wood specimens using the complete chloroplast genome of three *Pterocarpus* species. *Planta* **2019**, *250*, 95–104. [CrossRef]
49. Li, Y.; Tong, Y.; Xing, F. DNA barcoding evaluation and its taxonomic implications in the recently evolved genus *Oberonia* Lindl. (Orchidaceae) in China. *Front. Plant Sci.* **2016**, *7*, 1791. [CrossRef]
50. Smidt, E.C.; Páez, M.Z.; Vieira, L.N.; Viruel, J.; Baura, V.A.; Balsanelli, E.; de Souza, E.M.; Chase, M.W. Characterization of sequence variability hotspots in *Cranichideae plastomes* (Orchidaceae, Orchidoideae). *PLoS ONE* **2020**, *15*, e0227991. [CrossRef]
51. Cavalier-Smith, T. Skeletal DNA and the evolution of genome size. *Annu. Rev. Biophys. Bioeng.* **1982**, *11*, 273–302. [CrossRef]
52. Britten, R.J. Transposable element insertions have strongly affected human evolution. *Proc. Natl. Acad. Sci.* **2010**, *107*, 19945–19948. [CrossRef]
53. Chen, J.; Wang, F.; Zhou, C.; Ahamd, S.; Zhou, Y.; Li, M.; Liu, Z.; Peng, D. Comparative Phylogenetic Analysis for *Aerides* (Aeridinae, Orchidaceae) Based on Six Complete Plastid Genomes. *Int. J. Mol. Sci.* **2023**, *24*, 12473. [CrossRef]
54. Zhou, C.Y.; Zeng, M.Y.; Gao, X.; Zhao, Z.; Li, R.; Wu, Y.; Liu, Z.J.; Zhang, D.; Li, M.H. Characteristics and Comparative Analysis of Seven Complete Plastomes of *Trichoglottis* sl (Aeridinae, Orchidaceae). *Int. J. Mol. Sci.* **2023**, *24*, 14544. [CrossRef]
55. Zhao, Z.; Zeng, M.Y.; Wu, Y.W.; Li, J.W.; Zhou, Z.; Liu, Z.J.; Li, M.H. Characterization and Comparative Analysis of the Complete Plastomes of Five *Epidendrum* (Epidendreae, Orchidaceae) Species. *Int. J. Mol. Sci.* **2023**, *24*, 14437. [CrossRef]
56. Kocyan, A.; Endress, P.K. Floral structure and development of *Apostasia* and *Neuwiedia* (Apostasioideae) and their relationships to other Orchidaceae. *Int. J. Plant Sci.* **2001**, *162*, 847–867. [CrossRef]
57. Chase, M.W. Classification of Orchidaceae in the age of DNA data. *Curtis's Bot. Mag.* **2005**, *22*, 2–7. [CrossRef]
58. Cameron, K.M.; Chase, M.W.; Whitten, W.M.; Kores, P.J.; Jarrell, D.C.; Albert, V.A.; Yukawa, T.; Hills, H.G.; Goldman, D.H. A phylogenetic analysis of the Orchidaceae: Evidence from *rbcL* nucleotide sequences. *Am. J. Bot.* **1999**, *86*, 208–224. [CrossRef]